iScience

CellPress
OPEN ACCESS

Article

Stimulating both eyes with matching stimuli enhances V1 responses

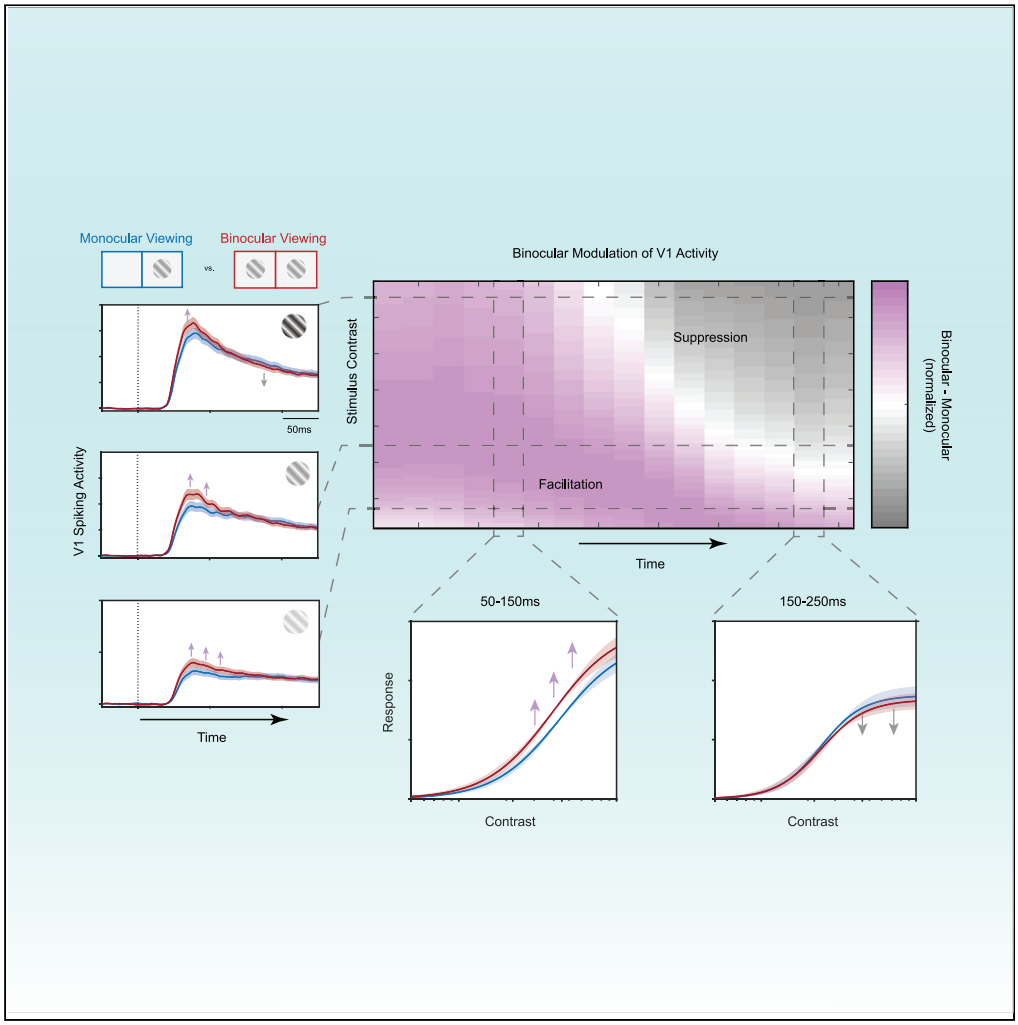

Blake A. Mitchell, Kacie Dougherty, Jacob A. Westerberg, Brock M. Carlson, Loïc Daumail, Alexander Maier, Michele A. Cox

michele.a.cox@gmail.com (M.A.C.)
blake.a.mitchell@vanderbilt.edu (B.A.M.)

Highlights

Binocular facilitation in primary visual cortex (V1) is contrast dependent

Lower contrasts result in greater binocular facilitation overall

Suppression follows initial facilitation of binocular response in V1

Contrast modulates both facilitation duration and suppression magnitude

Mitchell et al., iScience 25, 104182
May 20, 2022
https://doi.org/10.1016/j.isci.2022.104182

iScience

CellPress
OPEN ACCESS

Article

Stimulating both eyes with matching stimuli enhances V1 responses

Blake A. Mitchell,[1,4,*] Kacie Dougherty,[2] Jacob A. Westerberg,[1] Brock M. Carlson,[1] Loïc Daumail,[1] Alexander Maier,[1] and Michele A. Cox[3,*]

SUMMARY

Neurons in the primary visual cortex (V1) of primates play a key role in combining monocular inputs to form a binocular response. Although much has been gleaned from studying how V1 responds to discrepant (*dichoptic*) images, equally important is to understand how V1 responds to concordant (*dioptic*) images in the two eyes. Here, we investigated the extent to which concordant, balanced, zero-disparity binocular stimulation modifies V1 responses to varying stimulus contrast using intracranial multielectrode arrays. On average, binocular stimuli evoked stronger V1 activity than their monocular counterparts. This binocular facilitation scaled most proportionately with contrast during the initial transient. As V1 responses evolved, additional contrast-mediated dynamics emerged. Specifically, responses exhibited longer maintenance of facilitation for lower contrast and binocular suppression at high contrast. These results suggest that V1 processes concordant stimulation of both eyes in at least two sequential steps: initial response enhancement followed by contrast-dependent control of excitation.

INTRODUCTION

Neurons in primary visual cortex (V1) play a key role in combining monocular information to produce a stable, binocular percept (Barton, 2004). Neurophysiological studies have provided rich insight into the flow of monocular signals and emergence of binocular responses within the primary visual pathway (Bishop and Pettigrew, 1986; Blake and Wilson, 2011; Burkhalter and Essen, 1986; DeAngelis and Newsome, 1999; Ghose and Ts'O, 1997; Henriksen et al., 2016; Horton, 2006; Lehky and Maunsell, 1996; Livingstone and Tsao, 1999; Maunsell and Essen, 1983; Pack et al., 2003; Parker et al., 2016; Parker and Cumming, 2001; Poggio, 1995; Poggio and Fischer, 1977; Schroeder et al., 1990; Smith et al., 1997; Yang et al., 2011). However, many studies of binocular combination have been geared toward understanding how the visual system responds to images that are somewhat discrepant between the two eyes, i.e., *dichoptic* viewing conditions. Less is understood about how V1 responds under *dioptic* viewing conditions, where binocular images are physically identical and fall on corresponding retinal positions.

As a matter of subjective experience, the advantages of viewing the same image with both eyes are somewhat elusive (Levelt, 1965). The simple experiment of opening and closing one eye does not elicit a dramatic change in perception. Yet, decades of research have revealed a binocular advantage in numerous psychophysical experiments (For review, see Blake et al., 1981; Blake and Fox, 1973). Psychophysical gains in performance under binocular viewing are commonly referred to as "binocular summation" (e.g., Cagenello et al., 1993). It has now been well established that binocular summation extends beyond what would be expected from having an additional detector (i.e., probability summation) (For meta-analysis, see Baker et al., 2018; Matin, 1962; Pirenne, 1943). Thus, it is likely that binocular summation is facilitated by a neural interaction.

The neurophysiological basis for binocular summation is thought to be an enhancement of neural responses along the primary visual pathway (Blake and Fox, 1973). Electrophysiological and neuroimaging techniques have demonstrated neural binocular summation in human V1 (Apkarian et al., 1981; Heravian et al., 1990; Hou et al., 2020; Moradi and Heeger, 2009; Pardhan et al., 1990). Although enhanced compared to responses to just one eye, V1 binocular responses are typically much less than the sum of comprising

[1]Department of Psychology, Vanderbilt Brain Institute, Vanderbilt Vision Research Center, Vanderbilt University, Nashville, TN 37240, USA

[2]Princeton Neuroscience Institute, Princeton University, Princeton, NJ 08544, USA

[3]Center for Visual Science, University of Rochester, Rochester, NY 14627, USA

[4]Lead contact

*Correspondence: michele.a.cox@gmail.com (M.A.C.), blake.a.mitchell@vanderbilt.edu (B.A.M.)

https://doi.org/10.1016/j.isci.2022.104182

monocular responses (Ates et al., 2006; Giuseppe and Andrea, 1983; Heravian et al., 1990; Moradi and Heeger, 2009), akin to our experience of seeing with two eyes. The mechanisms of this sublinear/partial summation are not completely understood. However, modern models of binocular combination and theoretical frameworks for neural response normalization have made great inroads into the regulatory processes that facilitate and control binocular summation (Blake, 1989; Carandini and Heeger, 2012; Ding and Levi, 2021; Georgeson and Sengpiel, 2021; Hou et al., 2020; Ling and Blake, 2012; Meese et al., 2006; Said and Heeger, 2013). Foundational to such models is the parameter of stimulus contrast.

V1 neurons respond to a dynamic range of visual contrasts (Clatworthy et al., 2003). The relationship between stimulus contrast and a V1 neuron's response is typically well-described by a sigmoidal contrast response function (CRF) (Albrecht and Hamilton, 1982; Ohzawa et al., 1985; Sengpiel and Blakemore, 1994). By measuring the 'shifts' in the contrast-response relationship from one sensory condition to the next, experimenters have distinguished contrast-dependent and contrast-independent mechanisms that control V1 excitation (Heuer and Britten, 2002; Sengpiel et al., 1998). For example, the addition of an orthogonal grating in the opposite eye suppressed V1 neurons in a manner that shifted the CRF down along the response axis rather than the contrast axis. To the best of our knowledge, shifts in V1's CRF under the much more common visual experience of dioptic stimulation have not been fully characterized using multiunit electrophysiological methods.

Here, we studied the time-varying relationship between V1 binocular (dioptic) response modulation and stimulus contrast. We found that V1 population spiking activity was overall greater for binocular stimulation than for monocular stimulation, but binocular responses were considerably less than the left and right eye responses summed. The relationship between binocular modulation and stimulus contrast was dynamic. V1 binocular responses exhibited at least two sequential steps of gain modulation over monocular viewing: initial, rapid (50-100 ms) summation that was more contrast-invariant followed by slower, contrast-dependent processing, all within the timeframe of a typical fixation (250 ms; Salthouse and Ellis, 1980).

RESULTS

We were interested in determining how V1 activity differs between stimulating one eye versus stimulating both eyes with the same image as a function of contrast. To find out, we presented sinusoidal, achromatic gratings through a mirror stereoscope (Figure 1A) either monocularly or binocularly (Figure 1B) to fixating monkeys. Gratings varied in Michelson contrast between trials [0, 0.20-0.225, 0.40-0.45, and 0.80-0.90]. We used microelectrode arrays to simultaneously record extracellular voltages at multiple V1 sites. Thresholding the voltage at each site yielded a measure of neuronal activity (discretized multiunit, see STAR Methods for details). For each unit, we distinguished the eye that drove V1 activity the most as the dominant eye (DE; Figure 1C, dark blue) compared to the nondominant eye (NDE; Figure 1C, light blue).

Sampling in this study varied with monkey and condition (Table 1). As a result, population measures of neuronal activity reported below include a varying number of units from each monkey depending on the conditions being considered. For transparency, single-animal results are provided in tables or supplemental figures. Potential consequences of sampling-bias, which is not uncommon for studies of this kind, are considered in Discussion.

Binocular V1 responses exceed the average of monocular responses

Prior neurophysiological and imaging studies found that binocular responses constitute less than the linear sum of the converging left and right eye signals (Apkarian et al., 1981; Moradi and Heeger, 2009; Smith et al., 1997). We were curious to see if this was the case for our data as well.

Figure 1D shows each unit's mean binocular (BIN) responses (0-250 ms) plotted against the sum of its respective monocular responses (DE + NDE). The unity diagonal represents the expected binocular response if binocular summation is linear. Across our sample of multiunits (Table 1), binocular responses were approximately 56% of the summed monocular responses on average (low contrast, *linear regression slope*, $M = 0.55$, $SE = 0.011$, 95% *CI* [0.52,0.57], $p = 1.7378e^{-130}$; med contrast, $M = 0.56$, SE = 0.009, 95% *CI* [0.54,0.58], $p = 7.0530e^{-173}$; high contrast, $M = 0.57$, $SE = 0.009$, 95% *CI* [0.55,0.59], $p = 5.8719e^{-177}$, see Table 2 for breakdown by animal; see also Figure S2) and approximately 82% of the quadratic sum. To control for variance in maximum firing rate between units, we calculated an additivity index at each contrast. The additivity index was derived by dividing the mean binocular response of each unit by the

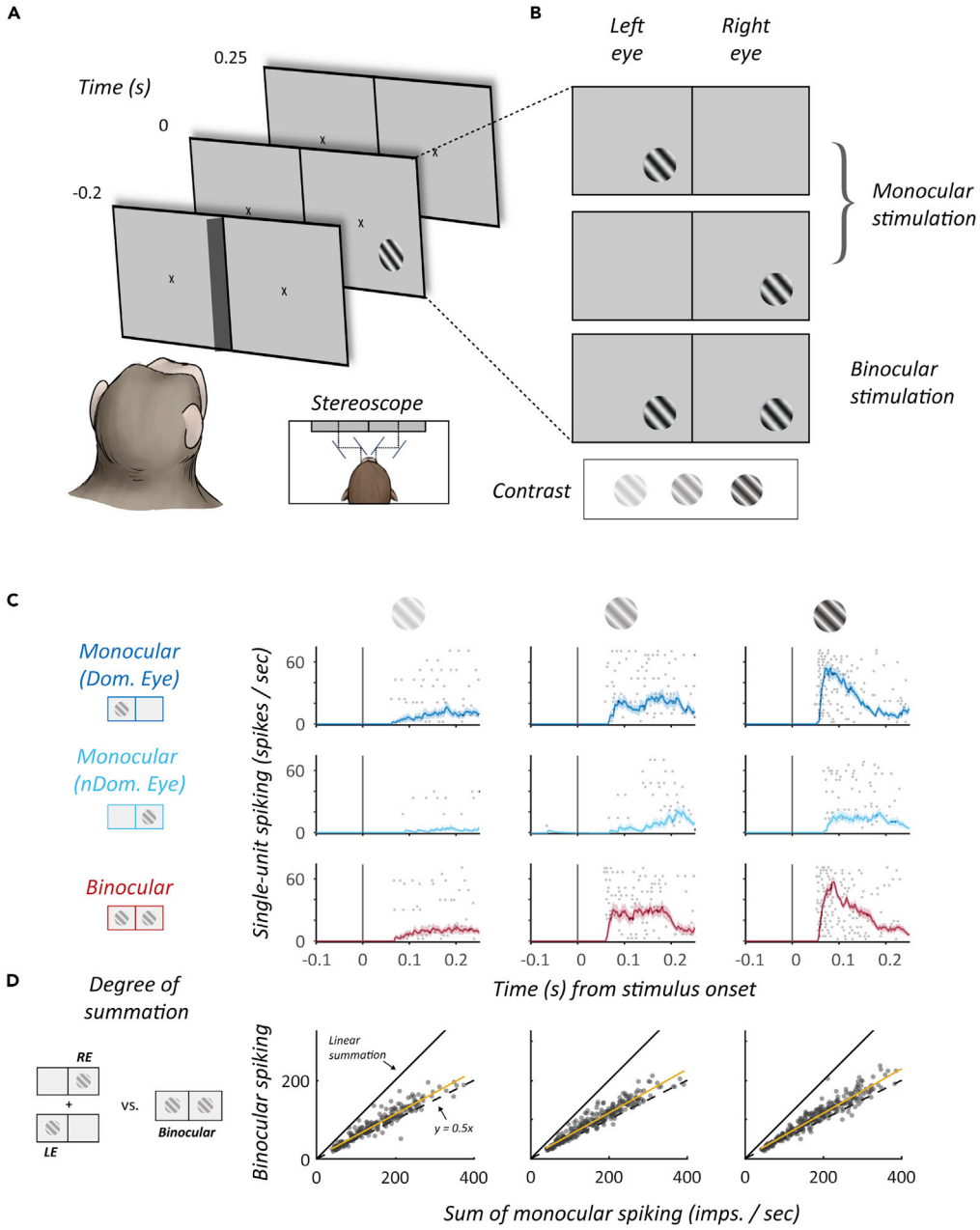

Figure 1. Experimental design

(A) Paradigm. Monkeys fixated while viewing static sinusoidal gratings through a mirror stereoscope. Stimuli covered the previously mapped receptive field location (dashed circle) for 250 ms while spiking responses were recorded from V1.

(B) Stimulus conditions. Gratings appeared either in the left eye (monocular), the right eye (monocular), or both eyes simultaneously (binocular). Orientation, size, and spatial frequency of gratings were held constant throughout each experiment. Gratings varied in Michelson contrast ([0], [0.20-0.22], [0.40-0.45], [0.80-0.90]) between trials.

(C) Raster plots (each dot is a spike, trials across vertical dimension) from an example unit for each type of stimulation (row) at each contrast (column) with superimposed spike density functions (shaded region represents +/− SEM). The eye that drove neural activity most vigorously was designated as the dominant eye (darker blue, top).

(D) Sublinear binocular combination. Mean firing rates (N = 314 units, 234 in monkey E) to binocular stimulation are plotted against the sum of monocular firing rates (left + right eye). Solid black line represents linear summation. Dashed black line represents y = 0.5×. Binocular responses were generally less than the arithmetic sum of their monocular counterparts at each contrast level and in both monkeys.

Table 1. Subject and Sample information

Subject	Sessions	Units	Low contrast	Med contrast	High contrast	CRFs
"E"	14	234	234	234	234	234
"I"	5	80	14	74	80	8
Pooled	19	314	248	308	314	242

sum of its comprising monocular responses [$BIN_{\mu}/\Sigma(LE_{\mu}+RE_{\mu})$]. An index value of 1 signifies that the binocular response was equivalent to the sum of comprising monocular responses. Similar to the slope coefficients, the mean additivity indexes were less than 1 but greater than 0.5 (low, M = 0.58, SD = 0.09, 95% CI [0.57,0.59]; med, M = 0.59, SD = 0.08, 95% CI [0.58,0.60]; high, M = 0.58, SD = 0.07, 95% CI [0.57,0.59]). Additivity indices did not significantly differ across contrast (*Mixed model*, F (869, 1) = 1.64, p = 0.2008). Thus, at the level of V1 population spiking, binocular responses show sublinear summation.

Facilitation of V1 spiking responses to balanced binocular stimulation

The aforementioned analysis replicated previous findings, showing that V1 responses tend to increase whenever a stimulus is shown to both eyes rather than one eye alone (akin to binocular summation). Given this expectation of a larger binocular response, another popular measure is to compare binocular stimulation to stimulation of whichever eye evokes the stronger response. We thus quantified this effect as well. To do so, we computed an index of "binocular modulation" as the difference in mean spiking response (0-250 ms) when both eyes are stimulated, referenced to the strongest monocular (dominant eye, DE) response (see STAR Methods and Figure 2A).

Binocular modulation index values above zero indicate binocular facilitation, whereas values below zero indicate binocular suppression. For each unit, we first pooled the data across contrast levels to achieve a grand average of V1 binocular modulation. We derived mean spiking responses over 250 ms (full duration of stimulus presentation). Figure 2B displays the grand average binocular modulation index for each unit. Across the population, binocular modulation was significantly greater than zero (M = 0.057, SD = 0.067, *paired t-test*, t (313) = 14.95, p < 0.001, *Cohen's d* = 0.843, see Table 3 for breakdown by animal). More than two thirds of V1 units (219 units, 69.7%) were overall facilitated when both eyes viewed the same image relative to monocular viewing.

Next, we examined the extent to which contrast modifies binocular modulation. Figure 2C shows the binocular response (mean spiking from 0 to 250 ms) of each unit against its dominant eye response as a function of stimulus contrast. Distributions of binocular modulation values are shown in the corner histograms. We found that binocular modulation varied across stimulus contrast (*Mixed model: N = 314*, F (1, 869) = 15.55, p < 0.001; see Table 3 for breakdown by animal). Binocular modulation was strongest for low contrast (M = 0.034, SD = 0.081, *paired t test* H_a $\mu > 0$, t (247) = 6.62, p < 0.001, *Cohen's d* = 0.42) and medium contrast (M = 0.034, SD = 0.072, *paired t test* H_a $\mu > 0$, t (307) = 8.32, p < 0.001, *Cohen's d* = 0.47) but weakest for high contrast (M = 0.020, SD = 0.070, *paired t test* H_a $\mu > 0$, t (313) = 5.10, p < 0.001, *Cohen's d* = 0.29). Although V1 spiking was predominantly facilitated over 250 ms of binocular stimulation, this boost in activity was attenuated by stimulus contrast.

Contrast dependency of facilitation across time

Informed by previous work (Cox et al., 2019), we suspected binocular facilitation in V1 to be transient, i.e., not lasting the entire 250 ms of stimulus viewing. However, the contrast dependency of this dynamic remains unknown. To investigate the temporal rise and decay of facilitation across contrast, we created spike density functions (SDFs) for monocular and binocular V1 responses and compared them across time. For this analysis, we limited our sample to units for which we had balanced observations for pairwise comparisons between contrasts (N = 242 units, 234 from monkey E, see Table 1).

Figure 3A displays the population SDFs as a function of stimulus contrast (For individual monkey data, see Figures S4A and S5B). Below each plot is the mean difference in spiking between monocular and binocular stimulation, normalized within-unit for three levels of contrast. Time points where binocular facilitation (above zero) was significant are indicated by a horizontal black line above the delta response (*two-way paired t-test*, p < 0.001). This time varying SDF analysis revealed that the magnitude of binocular facilitation

Table 2. Linear regression

Subject	Contrast	Estimate	SE	95% CI Lower	95% CI Upper	Student's t	p
"E"	Low	0.5504	0.0015	0.5278	0.5730	48.0209	<0.001
	Med	0.5567	0.0112	0.5467	0.5788	49.7850	<0.001
	High	0.5667	0.0116	0.5439	0.5896	48.7941	<0.001
"I"	Low	0.6050	0.0712	0.4499	0.7601	0.00391	0.9695
	Med	0.5424	0.0241	0.4945	0.5904	22.5344	<0.001
	High	0.5400	0.0185	0.5032	0.5769	29.1959	<0.001

Slope coefficients for additivity across contrast.

varied as a function of time at all three contrast levels. Specifically, binocular facilitation was largest at an early phase of the response and decreased over time. To further quantify this effect, we calculated the binocular modulation index over sixteen sequential temporal windows. As expected, the binocular modulation index varied significantly with time (medium contrast, *rmANOVA*, F (15, 3525) = 150, p < 0.001, n^2_G = 0.190; see also Figure S3).

We next estimated the magnitude of facilitation at the transient peak of V1 responses as a function of contrast. Peak magnitude varied across stimulus contrast, (*rmANOVA*, F (2, 482) = 24.0, p < 0.001, n^2_G = 0.035; Figure 3B – *top*). Low contrast facilitation exhibited peak magnitudes (M = 0.28, SD = 0.14) significantly lower than medium (M = 0.34, SD = 0.16) and high contrast (M = 0.35, SD = 0.22) peaks (low vs medium contrast, *post hoc test*, t (241) = −5.74, $p_{Bonferonni}$ < 0.001, *Cohen's d* = −0.37; low vs. high contrast, *post hoc test*, t (247) = −6.15, $p_{Bonferonni}$ < 0.001, *Cohen's d* = −0.39). Peak magnitude of facilitation at medium and high contrast were not statistically different (*post hoc test*, t (241) = −1.53, $p_{Bonferonni}$ = 0.36). See Table 4 for within-subject pairwise comparisons.

Finally, we measured the duration of facilitation across contrasts. For each unit, duration of facilitation was defined as the length in samples between the peak magnitude of facilitation (as previously described) and the point at which the delta response crossed zero (see STAR Methods for details). We found that duration of facilitation varied across contrast (*rmANOVA*, F (2, 482) = 4.74, p = 0.009, n^2_G = 0.012; Figure 3B – *bottom*). Facilitation was maintained significantly longer at low contrast (*Median* = 115.0 ms, *SD* = 63.3) compared to medium (*Median* = *87.0 ms*, *SD* = 59.7) and high contrast (*Median* = 80.0 ms, *SD* = 62.3;*post hoc test*, low vs. medium, t (215) = 2.80, $p_{Bonferonni}$ = 0.018, *Cohen's d* = 0.19; low vs. high, t (215) = 2.45, $p_{Bonferonni}$ = 0.045, *Cohen's d* = 0.17). Note, although both monkeys demonstrated the same trend, Monkey E's facilitation persisted for ~50 ms longer than Monkey I (Table 5). Duration of facilitation at medium and high contrast were not statistically different (*post hoc test*, medium vs. high, t (215) = −0.12, $p_{Bonferonni}$ > 0.9999).

V1 responses at higher contrasts transition from facilitation to suppression

Results thus far suggest that V1 binocular facilitation is a transient event that evolves over the time course of stimulation in a contrast-dependent manner. To further examine the dynamic relationship between binocular modulation and contrast, we interpolated the contrast responses of each unit by fitting measured data with the Naka-Rushton function (Figure 4A, see STAR Methods). V1 units with at least four contrast-level data points (234 units in Monkey E, 8 units in Monkey I, see Table 1) were used for fitting contrast response functions (CRFs). Monocular and binocular CRFs were computed over sixteen sequential temporal windows of the V1 spiking response. Windows were 100 ms in length, each sliding by 10 ms forward in time from the preceding window.

To evaluate V1 CRFs at the population level, we generated average curves for each condition using the mean parameters (and their upper and lower bounds). Figure 4B plots the mean parameter-generated binocular and monocular CRFs as a function of time. Color and contour of the floor reflects the normalized difference between each CRF pair as it evolves over time (pink = facilitation; white = no difference, gray = suppression. Figure 4C displays three windows (50-15 0 ms, 100-200 ms, and 150-250 ms) for closer inspection. We designated these windows as early, intermediate, and late, respectively. In the early period of the response (50-150 ms), binocular facilitation appeared the most proportional to stimulus contrast. In the

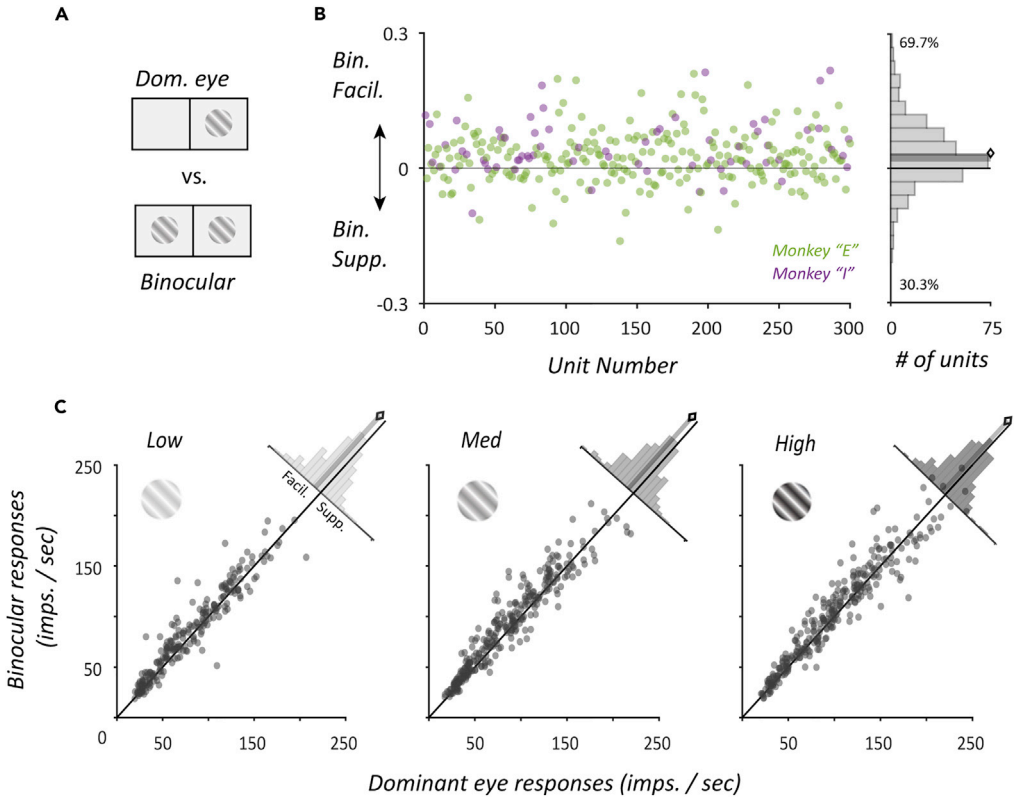

Figure 2. Facilitation of V1 spiking responses to balanced binocular stimulation

(A) We computed binocular modulation index to compare a unit's strongest monocular response (its preferred eye) to its binocular response over the full stimulus duration (0-250 ms). Values above 0 signify binocular facilitation, whereas values below 0 signify binocular suppression.

(B) Within-unit average (across contrast) binocular modulation index (M = 0.057, SD = 0.067, N = 314 [234 from Monkey "E", shown in green]). Distribution to the right shows that most V1 units were facilitated (shaded region encasing 95% CI, diamond marks the mean).

(C) Binocular modulation as a function of contrast. In each panel, a unit's binocular response is plotted against its strongest monocular response. Distribution of the binocular modulation index is shown in the corner histogram; the gray shaded region represents the 95% confidence interval; the black diamond marks the mean of the distribution. Facilitation was observed in most V1 units and at each contrast tested.

intermediate period (100-200 ms), binocular facilitation was diminished at high contrast. By the late period (150-250 ms), binocular facilitation had relinquished entirely. Instead, the late period V1 CRF exhibited *binocular suppression* at medium and high contrast. Given sampling, this specific population-level analysis is biased toward monkey E (234 units in Monkey E, 8 units in Monkey I, see Table 1); therefore, we additionally examined single-penetration from each subject individually (Figures S4B and S5C). These penetrations exhibit the same overall trend as the population analysis, although with larger standard error given the lower number of units.

V1 binocular facilitation predominantly resembles response-gain

We next evaluated the contrast-response relationship in the context of simple forms of gain and gain-control. Two hypothetical types of gain can be gleaned from shifts in the CRF (Ling and Carrasco, 2006; Martinez-Trujillo and Treue, 2002; Ohzawa et al., 1985; Sengpiel et al., 1998; Sengpiel and Blakemore, 1994; Thiele et al., 2009). Response-gain is characterized by vertical shifts in V1's CRF, indicating that responses increased with contrast by a constant scaling factor. On the other hand, contrast-gain is characterized by horizontal shifts in V1's CRF, indicating a contrast-response relationship that depends on contrast.

To quantitatively evaluate which type of gain (response vs. contrast-gain set) is prevalent at the population level, we directly compared models that isolate the effects of response-gain and contrast-gain. In this

Table 3. Paired Samples *t*-test

Subject	Contrast	Bayes factor$_{10}$[a]	Student's t	Df	p	Cohen's d
"E"	Grand	5.19e+29	13.99	233	<0.001	0.914
	Low	4.43e+6	6.13	233	<0.001	0.401
	Med	8.21e+6	6.25	233	<0.001	0.408
	High	121	3.74	233	<0.001	0.245
"I"	Grand	695497.5	6.11	79	<0.001	0.683
	Low	11.7	3.04	13	0.005	0.811
	Med	525811.6	6.09	73	<0.001	0.708
	High	104.4	3.68	79	<0.001	0.411

Binocular modulation index (0-250ms) across contrast.
Note. H_a μ Measure > 0.
[a]Cauchy prior 0.707.

procedure, we fixed the parameters of the Naka-Rushton equation to that of the dominant eye. We then introduced a single free parameter (G) to either multiply response (response-gain model, eq. 1 in Figure 5A) or contrast (contrast-gain model, eq. 2 in Figure 5A). Finally, we fit the mean response (over 100 ms windows of the response) from the binocular condition with each model and compared their performance.

Figure 5B shows the population-level fitted binocular responses for the two models at the early, intermediate, and late phase of the response, with goodness of fit for each model plotted below (see Table 6 for breakdown by animal). Both response-gain and contrast-gain set model performance varied significantly across time (response-gain, *rmANOVA*, F (2,482) = 17.8, p < 0.001, n^2_G = 0.030; contrast-gain, *rmANOVA*, F (2,482) = 40.0, p < 0.001, n^2_G = 0.065). Response-gain performed best (R^2 = 0.90, *95% CI* [0.88, 0.92]) and significantly better than contrast-gain (R^2 = 0.87, *95% CI* [0.85, 0.89]) during the early phase (50-150 ms, window 5) of the response (*paired t-test*, t (241) = 2.84, p = 0.00491, *Cohen's d* = 0.18). During the intermediate phase (100-200 ms, window 10), response-gain and contrast-gain performances were comparable (response-gain, R^2 = 0.86, *95% CI* [0.84, 0.89]; contrast-gain, R^2 = 0.84, *95% CI* [0.82, 0.87]). In the late phase (150-250 ms, window 15), performance of these simple models of gain decreased overall (response-gain, R^2 = 0.81, *95% CI* [0.78, 0.84]; contrast-gain, R^2 = 0.73, *95% CI* [0.69, 0.77]). Recall that the late stage of the binocular response exhibited suppression (far right Figure 4B). Binocular suppression of V1's CRF was better captured by response-gain set (*paired t-test*, t (241) = 6.26, p < 0.001, *Cohen's d* = 0.40). We note that binocular suppression unfolded differently across time between the two monkeys (see Figure S4B). However, in both cases, contrast-dependent suppression was observed following facilitation. Figure 5C shows the normalized parameter differences (R_{max} and C_{50}) of the CRF pairs across time. As expected, differences in R_{max} corresponded with response-gain performance, whereas differences in C_{50} corresponded with contrast-gain performance.

To summarize, response-gain (increase in R_{max}) under binocular stimulation was most prominent at the initial peak V1 response (50-100 ms). Contrast-dependent decay of facilitation disrupted response-gain, eventually suppressing V1's CRF. Although performance of both models was markedly reduced in the late phase (150-250 ms) of the V1 response, the binocular suppression we observed was better explained by a reduction to firing rates, i.e., response-gain control.

DISCUSSION

We report that V1 spiking responses are predominantly *facilitated* (i.e., enhanced) by adding the same stimulus at a matching retinotopic position in the other eye. This binocular facilitation was centered around the transient peak of the V1 response. In line with earlier reports (Cox et al., 2019), we find that the later-sustained phase of binocular V1 responses approaches its monocular counterpart, eradicating—and at some contrast levels even reversing—any binocular facilitation. We show that initial binocular processing in V1 is better explained by a model of response-gain as opposed to contrast-gain. However, we found that simple models of contrast-response relationships break down as more complex, contrast-dependent dynamics emerge in the sustained V1 response.

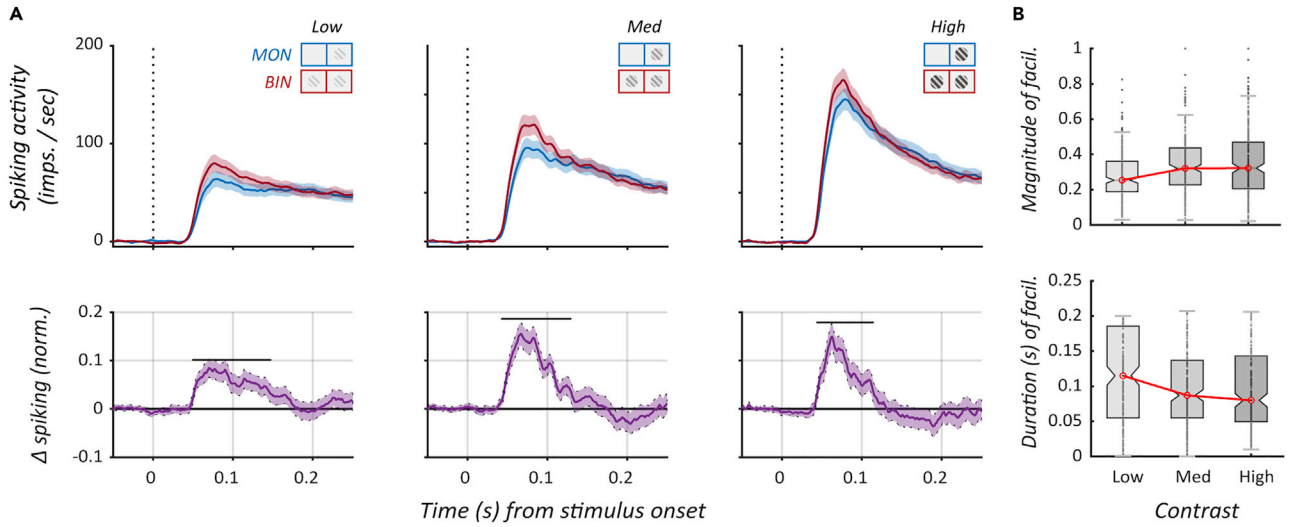

Figure 3. Contrast dependency of V1 binocular facilitation across time

(A) Top - Population spike density functions (SDFs) for monocular (blue) and binocular stimulation (red) are shown for three contrast levels ([0.22, 0.45, and 0.90]). Dotted line at zero represents stimulus onset. Shaded region represents 95% CI. Bottom - Difference between the SDFs (BIN – MON) across time, calculated within-unit and normalized to each unit's maximum binocular response. Shaded region represents 95% CI. Note that facilitation was limited to the early phase of the response.

(B) Top – Peak magnitude of facilitation increased as a function of contrast. Data points are shown in black (dots). Boxplot upper and lower edges indicate the 25th and 75th percentiles, respectively. Red line connects the median value (red circle) of each boxplot. Whiskers extend to the most extreme data points that are not considered outliers. Bottom – duration of facilitation systematically decreased as a function of contrast. Same conventions as mentioned before.

Relation to prior literature

Research into the origins of psychophysical gains of binocular vision has pointed to binocular interactions along the primary visual pathway (Blake and Fox, 1973). Early investigations of binocular interactions found great diversity in how V1 simple and complex cells modulate under binocular stimulation (Hubel and Wiesel, 1962). Responses of binocularly activated single cells in striate cortex are shown to be either greater than the sum of monocular responses, greater than the preferred monocular response, or less than monocular responses (Barlow et al., 1967; Burns and Pritchard, 1968; Hubel and Wiesel, 1962; Pettigrew et al., 1968; Poggio and Fischer, 1977). We now understand that this diversity is functional. The type of binocular interactions in single neurons rely chiefly, among other factors, on the compatibility between retinal disparity of the stimulus and the shape of a given cell's receptive field (Anzai et al., 1999; Barlow et al., 1967; Bishop and Pettigrew, 1986; Cumming and DeAngelis, 2001; Freeman and Ohzawa, 1990; Hubel and Wiesel, 1962; Poggio and Fischer, 1977; Smith et al., 1997; Nikara, 1972).

Binocular interactions have also been measured in humans and animals at the spatial and temporal resolutions afforded by EEG and neuroimaging. Visual-evoked responses to binocular stimulation are at least 25% greater than the preferred eye or the average of the two monocular responses (Apkarian et al., 1981; Heravian et al., 1990; Sclar et al., 1986; Summa et al., 1997). Similarly, the BOLD signal in V1 is modestly greater for congruent binocular gratings compared to monocular gratings (Moradi and Heeger, 2009).

Here, we report V1 binocular interactions at the intermediate level of neural population spiking activity using multiunit electrophysiology. We found that V1 binocular responses constituted less than the arithmetic sum of left and right eye responses (sublinear/partial binocular summation). At the same time, V1 binocular spiking was higher than that of the population's preferred eye (binocular facilitation). This overall increase in neural population activity for binocular stimulation is in line with the single-neuron experiments in rodents (Longordo et al., 2013; Zhao et al., 2013), cats (Grünau, 1979; Grünau and Singer, 1979; Hubel and Wiesel, 1962), monkeys (Poggio and Fischer, 1977), and is consistent with the idea that V1 neurons with near foveal receptive fields tend to show an excitatory bias towards zero-disparity (Poggio and Fischer, 1977). Yet, the magnitude of binocular facilitation was less than that reported in single neurons optimally stimulated with images placed at corresponding retinal positions (Burns and Pritchard, 1968). The magnitude of facilitation reported here is quantitatively closer to estimates from fMRI (Moradi and Heeger, 2009)

Table 4. Paired Samples *t*-test

Subject	Comparison	Mean difference	Bayes factor$_{10}$[a]	Student's t	df	P[b]	Cohen's d
"E"	Low – Med	−0.052	61573.529	−5.41	233	<0.001	−0.35
	- High	−0.071	547386.053	−5.86	233	<0.001	−0.38
	Med – High	−0.019	0.256	−1.60	233	0.34	−0.10
"I"	Low – Med	−0.157	1.319	−2.03	7	0.2461	−0.72
	- High	−0.085	0.734	−1.57	13	0.4198	−0.42
	Med – High	−0.018	0.352	0.33	7	0.9999	0.12

Peak magnitude of facilitation across contrast.
[a]Cauchy prior 0.707.
[b]Bonferroni adjusted p value.

and EEG (Harter et al., 1973). Population measurements contain neurons with different tuning preferences, which might – at least – partially explain this difference.

In addition to better spatial sampling of binocular interactions, we were also able to assess the temporal dynamics of neural binocular summation at behaviorally relevant timescales (Salthouse and Ellis, 1980). In a recent meta-analysis of psychophysical binocular summation, a negative correlation was found between psychophysical binocular summation and stimulus duration (Baker et al., 2018). That is, the magnitude of binocular summation effects tended to decrease with exposure time. For example, psychophysical binocular summation in orientation discrimination was shown to be greatest for a brief exposure time of 50 ms, which approached nonsignificance (indistinguishable from monocular stimulation) at durations of 100 ms or longer (Bearse and Freeman, 1994). We found that V1 spiking responses were transiently facilitated (50–150 ms) with peak magnitude of facilitation localized around the initial peak of the response (45–50 ms). In the sustained period of the response, binocular responses were comparable to (and even less than) monocular responses, akin to the invariance of perception when opening and closing one eye. Thus, the timescales of V1 binocular enhancement reported here are consistent with the timescales reported previously for behavioral performance gains and our subjective experience of binocular vision.

Our first set of findings thus seems well in line with previous findings and the psychophysical literature on binocular summation. This convergence of studies provides a strong base that we build our findings of contrast dependency on.

V1, contrast, and binocular gain-control

Contrast is a basic property of vision (Campbell and Robson, 1968) to which nearly all neurons in V1 increase in firing rates (Conway et al., 2002). When local contrast changes, V1 neurons adjust their dynamic range to meet the new local mean (Boynton, 2005; Ohzawa et al., 1985). This flexibility is often referred to as contrast-gain control and has been established as a fundamental operation throughout the primary visual pathway (Boynton, 2005).

Table 5. Paired Samples *t*-test

Subject	Contrast	Estimate (SD)	Comparison	Mean difference	Bayes factor$_{10}$[a]	Student's t	df	P[b]	Cohen's d
"E"	Low	106 (64.3)	Low - Med	12.1	1.93	2.28	211	0.036	0.16
	Med	88 (58.6)	- High	11.1	0.91	1.92	207	0.084	0.13
	High	81 (62.3)	Med - High	1.7	0.10	0.33	217	0.999	0.03
"I"	Low	53.5 (40.7)	Low - Med	36.0	3.41	2.30	7	0.081	0.81
	Med	24 (24.4)	- High	33.5	12.9	3.10	13	0.012	0.83
	High	21 (19)	Med - High	4.9	0.49	0.46	7	0.963	0.18

Duration (milliseconds) of facilitation across contrast.
Note. H_a μ Measure 1 – Measure 2 > 0.
[a]Cauchy prior 0.707.
[b]Bonferroni adjusted p value.

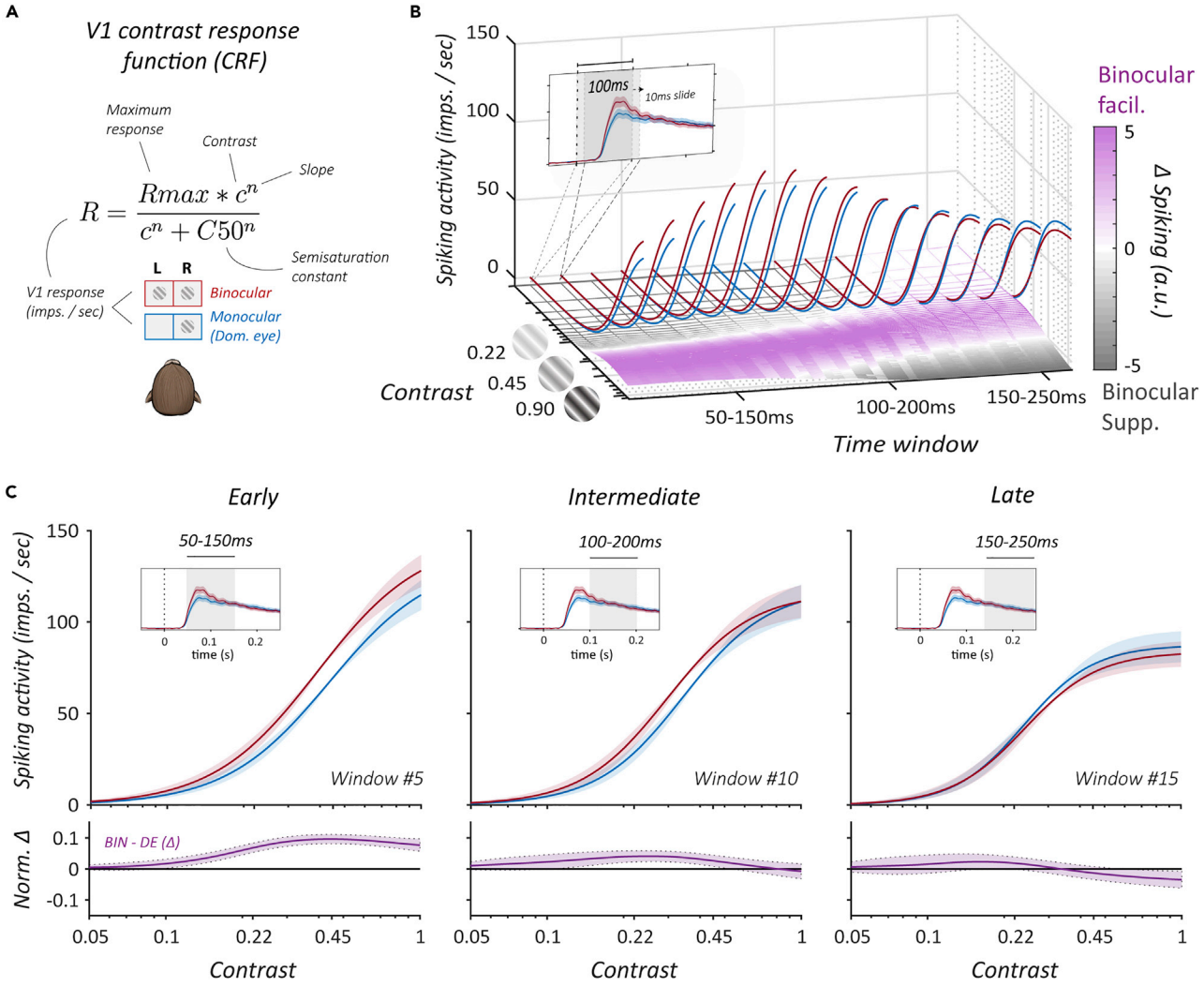

Figure 4. V1 responses at higher contrasts transition from facilitation to suppression

(A) Naka-Rushton h-ratio equation used to fit individual contrast response functions (CRFs). Mean parameters were then used to estimate monocular and binocular CRFs of the V1 population.

(B) Binocular and monocular CRFs were computed consecutively over 100 ms windows of the V1 response, sliding by 10 ms forward in time. Sixteen windows in total are shown along the y axis (x axis is contrast, z axis is spiking response). The floor of the plot reflects the difference between the CRF pairs across time. Color bar translates these differences into strength of facilitation (pink) or suppression (gray) (C) CRFs for three temporal windows pulled from A ([50–150 ms], [100–200 ms], and [150–250 ms]), designated as the early, intermediate, and late phase of the responses, respectively. Shaded region represents 95% CI of the parameters used to construct the curves. Facilitation appeared the most proportional to contrast in the early phase (50–150 ms). At the intermediate phase (100–200 ms) facilitation was diminished at high contrast. By the late phase (150–250 ms), facilitation was relinquished, giving way to binocular suppression at medium and high contrast.

A special type of contrast-gain control has been described for the transition from monocular to dichoptic viewing, i.e., when an *incompatible* image is 'added' to the other eye (Sengpiel and Blakemore, 1994). Such dichoptic stimulation has been shown to instigate inhibitory neural interactions that suppress the responses of V1 neurons, effectively shifting the V1 CRF downward along the y axis (Sengpiel and Blakemore, 1994). Our findings for *dioptic*, i.e., balanced binocular, stimulation show the opposite effect. We found that dioptic stimulation led to transient facilitation of V1 responses that resemble *response-gain*, expressed as an upward shift of the CRF along the y axis. Yet, binocular responses were still subject to some form of control as they did not constitute a linear sum of their constituting monocular parts. Previous empirical work has suggested that multiplicative gain control in cortical neurons can be similarly induced by either excitation or inhibition alone (Murphy and Miller, 2003). This suggests the possibility

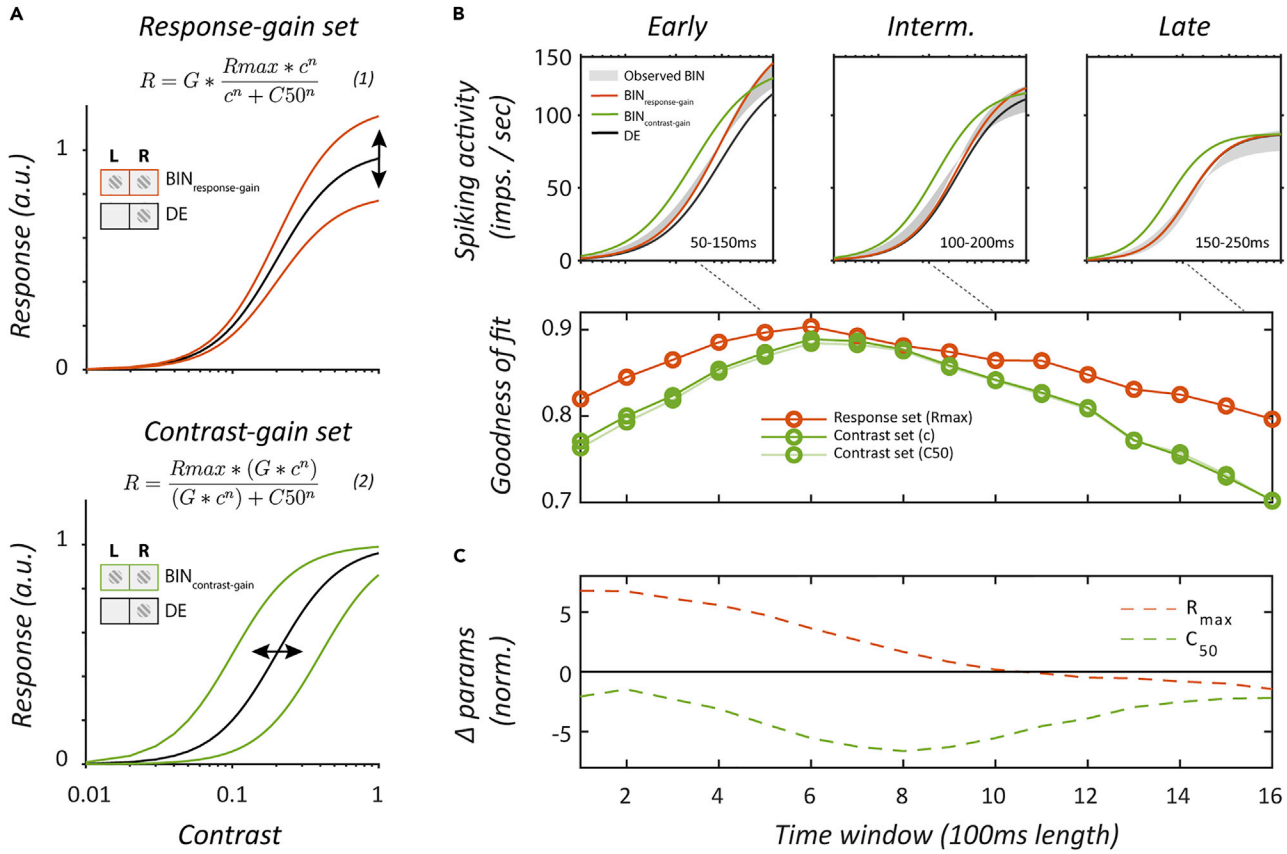

Figure 5. The effect of balanced binocular stimulation in V1 predominantly resembles a response-gain

(A) Models for how binocular stimulation interacts with contrast to modulate V1 responses. A single free parameter G multiplies either response (orange, response-gain) or contrast (green, contrast-gain) to fit binocular responses, whereas all other parameters are fixed to the monocular (dom. eye) condition.

(B) Top – model curves overlaid the 95% CI of the binocular CRF fit by the standard function. Bottom – goodness of fit (R^2) for both models as a function of time. We additionally tested an alternative model of contrast-gain set (light green) that multiplies the semi-saturation constant (c_{50}). Performance of the two contrast-gain set models was comparable.

(C) Difference (normalized) in the parameters R_{max} and C_{50} of the CRFs. Binocular stimulation transiently shifts V1's CRF upward in a manner that resembles response-gain before contrast-dependent dynamics shape the sustained response.

that one and the same mechanism—gain modulation of firing rates—may be responsible for the response control when the two images in the eyes either match or do not match. Future experiments that compare dioptic to dichoptic V1 responses at the same temporal resolution will be needed to test this hypothesis directly.

Relation to models of binocular combination

Although simple models of gain control are useful in evaluating contrast-response relationships, it is understood that the rules that govern binocular combination extend beyond a single parameter. Informed by decades of theoretical development and empirical work (Blake, 1989; Campbell and Green, 1965; Legge, 1984), the predictive power of modern models of binocular combination, such as the DSKL model (Ding and Sperling, 2006), have become progressively robust to a wide range of binocular viewing conditions (Ding et al., 2013a, 2013b; Ding and Levi, 2017, 2021; Huang et al., 2010; Yehezkel et al., 2016). Key to the success of such models has been the incorporation of multiple channels for reciprocal contrast-gain control to occur between the two eyes. Neural models of binocular combination employ similar formalisms and synergize well with the gain-control theory of binocular combination. In addition, they must account for known properties of visual neurons, such as the linear spatial summation of V1 simple cells, the nonlinearities of complex cells and spike generation, and the diversity in the interocular balance of inputs to a given cell. Notably, the two-stage model (Georgeson and Sengpiel, 2021), energy models (Fleet et al., 1996; Haefner and Cumming, 2008; Ohzawa et al., 1997; Read et al., 2002; Read and Cumming, 2003;

Table 6. Goodness of fit

		Early		Intermediate		Late	
Subject	Gain Model	R^2	95% CI	R^2	95% CI	R^2	95% CI
"E"	Response-gain	0.90	[0.88, 0.92]	0.87	[0.85, 0.89]	0.81	[0.78, 0.84]
	Contrast-gain	0.88	[0.86,0.90]	0.85	[0.82,0.87]	0.73	[0.69, 0.77]
"I"	Response-gain	0.78	[0.56,1.00]	0.77	[0.58, 0.96]	0.87	[0.80, 0.95]
	Contrast-gain	0.74	[0.50,0.96]	0.78	[0.56, 0.99]	0.86	[0.75, 0.97]

Simple models of binocular gain across temporal phases of V1 response.
Note. Naka-Rushton function fitted with three free parameters to units with at least four contrast levels.

Tanabe and Cumming, 2008), and binocular/interocular normalization (Chadnova et al., 2018; Hou et al., 2020; Ling and Blake, 2012; Moradi and Heeger, 2009; Tsang and Shi, 2008) have shown promise in accounting for the neural interactions that give rise to V1 binocular responses.

Results discussed in this paper are consistent with the contrast-gain control theory of binocular combination. Specifically, binocular facilitation in V1 was attenuated by high stimulus contrast, an explicit prediction of the DSKL model (Ding and Levi, 2021). We also report on the temporal dynamics of binocular modulation as a function of contrast. We found that the contrast-dependency of binocular modulation varied as a function of time. A potential implication of this finding is that binocular integration consists of sequential stages that can be operationally defined in terms of the V1 binocular contrast-response relationship. This implication could be further explored by evaluating existing neural models of binocular combination over sequential phases of the V1 response or by comparing model performance across varying levels of stimulus exposure. Based on the evolving contrast-response relationship we observed here, it is conceivable that the rate at which binocular response-gain decays in V1 could be parameterized.

Binocular response dynamics

Previously, we have shown that binocular responses in V1 exhibit at least two sequential steps that comprise initial facilitation followed by widespread differentiation between binocular concordance and discordance (Cox et al., 2019). Importantly, that work was specifically aimed at characterizing modulatory effects of the nondominant eye. Thus, unlike here, contrast in the nondominant eye always exceeded that of the dominant eye regardless of concordance or discordance in stimulus orientation. Results here focus on the much more common visual experience of dioptic situations.

We extend our previous work by revealing a relationship between the temporal dynamics of binocular modulation and stimulus contrast. Specifically, initial facilitation of V1 to dioptic stimulation resembled response-gain, characterized by an upward shift of V1's CRF. As V1 responses evolved, contrast dependency emerged. Contrast dependency was evidenced by the finding that contrast inversely correlated with facilitation duration, meaning that facilitation persisted longer for lower contrasts than higher contrasts. In addition, contrast positively correlated with suppression, such that V1 responses to high contrast binocular stimulation were lower than responses to monocular stimulation of the preferred eye. Finally, a model that assumes V1's binocular response multiplicatively scales with contrast (contrast invariant) explained the initial transient but varied significantly over the time course of the stimulus presentation. These findings suggest that binocular contrast combination is a dynamic process that involves multiple steps of processing: an initial, rapid process that is more contrast-invariant and a subsequent, slower process that is more contrast-dependent.

Limitations of the study

Data presented in this manuscript is drawn from multiple subjects but biased towards one. Therefore, population averages of spiking activity are influenced by one subject more than the other. Subject sampling-bias is not unusual for work of this kind. For transparency, units per subject and condition are detailed in tables and statistical tests throughout the manuscript, and individual subject data is presented in supplementary figures. Nevertheless, we must consider the implications for the generalizability of findings reported here. One possibility is that our observations and corresponding conclusions truly only apply to one individual subject and thus do not represent a general processing strategy of primates' visual cortex.

The observations that rest most firmly on data from a single animal are those pertaining to the shape of the CRFs and the temporal dynamics of contrast-dependent decay of binocular facilitation. In the latter case, there seems to be a slight difference in the timing of transition between contrast-dependent facilitation and suppression in one animal, which can be observed by comparing single-penetration data from each subject provided in supplement. Whether this is a true individual difference or a result of poor sampling is unclear. Future work that examines these or similar conditions in additional individuals will hopefully add weight to one interpretation or another.

Another caveat relating to the specific finding of contrast-dependent decay of binocular facilitation has to do with an inability to differentiate contrast-dependent effects from magnitude-dependent effects. Specifically, we report a contrast-dependent decay of initial binocular facilitation whereby higher contrasts drive a faster transition between facilitation and suppression of the binocular response compared to the monocular response. However, higher contrast stimuli also evoke more V1 spiking than lower contrasts stimuli when all other stimulus features are kept consistent. Therefore, an alternative explanation is that the magnitude of the initial transient itself determines the rate of decay of binocular facilitation. Thoughtfully designed future experiments might be necessary to distinguish between these two mechanisms.

STAR★METHODS

Detailed methods are provided in the online version of this paper and include the following:

- KEY RESOURCES TABLE
- RESOURCE AVAILABILITY
  - Lead contact
  - Materials availability
  - Data and code availability
- EXPERIMENTAL MODEL AND SUBJECT DETAILS
- METHOD DETAILS
  - Surgical procedures
  - Visual apparatus
  - Behavioral task
  - Neurophysiological procedure
  - Pre-processing of spiking activity
- QUANTIFICATION AND STATISTICAL ANALYSIS
  - V1 responses to monocular and binocular stimulation
  - Duration of binocular facilitation
  - Determining ocular dominance
  - Contrast response functions (CRFs)
  - Statistical analysis

SUPPLEMENTAL INFORMATION

Supplemental information can be found online at https://doi.org/10.1016/j.isci.2022.104182.

ACKNOWLEDGMENTS

This work was supported by NEI (P30EY008126, R01EY027402) and the Office of the Director (S10OD021771). B. A. M. and J. A. W. were supported by a training grant from NEI (T32EY007135) as was M.A.C (T32EY007125). J. A. W. was additonally supported by a fellowship from the NEI (F31EY031293). The authors would like to thank B. Williams, D. Richardson, I. Haniff, L. Toy, M. Feurtado, M. Maddox, M. Schall, R. Williams, and S. Motorny for technical support.

AUTHOR CONTRIBUTIONS

B. A. M., A. M., and M. A. C. designed the research. K. D., J. A. W., and M. A. C. performed research. B. A. M. analyzed the data. B. A. M. prepared visualizations. B. A. M., K. D., J. A. W., B. M. C., L. D., A. M., and M. A. C. wrote the manuscript.

DECLARATION OF INTERESTS

The authors declare no competing interests.

Received: September 14, 2021
Revised: February 18, 2022
Accepted: March 29, 2022
Published: May 20, 2022

REFERENCES

Albrecht, D.G., and Hamilton, D.B. (1982). Striate cortex of monkey and cat: contrast response function. J. Neurophysiol. *48*, 217–237. https://doi.org/10.1152/jn.1982.48.1.217.

Anzai, A., Ohzawa, I., and Freeman, R.D. (1999). Neural mechanisms for processing binocular information I. Simple cells. J. Neurophysiol. *82*, 891–908. https://doi.org/10.1152/jn.1999.82.2.891.

Apkarian, P., Levi, D., and Tyle, C.W. (1981). Binocular facilitation in the visual-evoked potential of strabismic amblyopes. Optom. Vis. Sci *58*, 820–830. https://doi.org/10.1097/00006324-198110000-00007.

Ates, K., Demirtas, S., and Goksoy, C. (2006). Binocular interactions in the Guinea pig's visual-evoked potentials. Brain Res. *1125*, 26–30. https://doi.org/10.1016/j.brainres.2006.10.016.

Baker, D.H., Lygo, F.A., Meese, T.S., and Georgeson, M.A. (2018). Binocular summation revisited: beyond √2. Psychol. Bull *144*, 1186–1199. https://doi.org/10.1037/bul0000163.

Barlow, H.B., Blakemore, C., and Pettigrew, J.D. (1967). The neural mechanism of binocular depth discrimination. J. Physiol. *193*, 327–342. https://doi.org/10.1113/jphysiol.1967.sp008360.

Barton, R.A. (2004). Binocularity and brain evolution in primates. Proc. Natl. Acad. Sci. U S A. *101*, 10113–10115. https://doi.org/10.1073/pnas.0401955101.

Bearse, M.A., and Freeman, R.D. (1994). Binocular summation in orientation discrimination depends on stimulus contrast and duration. Vis. Res *34*, 19–29. https://doi.org/10.1016/0042-6989(94)90253-4.

Bishop, P.O., and Pettigrew, J.D. (1986). Neural mechanisms of binocular vision. Vis. Res *26*, 1587–1600. https://doi.org/10.1016/0042-6989(86)90177-x.

Blake, R. (1989). A neural theory of binocular rivalry. Psychol. Rev. *96*, 145–167. https://doi.org/10.1037/0033-295x.96.1.145.

Blake, R., and Fox, R. (1973). The psychophysical inquiry into binocular summation. Percept Psychophys *14*, 161–185. https://doi.org/10.3758/bf03198631.

Blake, R., Sloane, M., and Fox, R. (1981). Further developments in binocular summation. Percept Psychophys *30*, 266–276. https://doi.org/10.3758/bf03214282.

Blake, R., and Wilson, H. (2011). Binocular vision. Vis. Res *51*, 754–770. https://doi.org/10.1016/j.visres.2010.10.009.

Boynton, G.M. (2005). Contrast gain in the brain. Neuron *47*, 476–477. https://doi.org/10.1016/j.neuron.2005.08.003.

Burkhalter, A., and Essen, D.V. (1986). Processing of color, form and disparity information in visual areas VP and V2 of ventral extrastriate cortex in the macaque monkey. J. Neurosci. *6*, 2327–2351. https://doi.org/10.1523/jneurosci.06-08-02327.1986.

Burns, B.D., and Pritchard, R. (1968). Cortical conditions for fused binocular vision. J. Physiol. *197*, 149–171. https://doi.org/10.1113/jphysiol.1968.sp008552.

Cagenello, R., Halpern, D.L., and Arditi, A. (1993). Binocular enhancement of visual acuity. J. Opt. Soc. Am. *10*, 1841. https://doi.org/10.1364/josaa.10.001841.

Campbell, F.W., and Green, D.G. (1965). Monocular versus binocular visual acuity. Nature *208*, 191–192. https://doi.org/10.1038/208191a0.

Campbell, F.W., and Robson, J.G. (1968). Application of fourier analysis to the visibility of gratings. J. Physiol. *197*, 551–566. https://doi.org/10.1113/jphysiol.1968.sp008574.

Carandini, M., and Heeger, D.J. (2012). Normalization as a canonical neural computation. Nat. Rev. Neurosci. *13*, 51–62. https://doi.org/10.1038/nrn3136.

Chadnova, E., Reynaud, A., Clavagnier, S., Baker, D.H., Baillet, S., and Hess, R.F. (2018). Interocular interaction of contrast and luminance signals in human primary visual cortex. Neuroimage *167*, 23–30. https://doi.org/10.1016/j.neuroimage.2017.10.035.

Clatworthy, P.L., Chirimuuta, M., Lauritzen, J.S., and Tolhurst, D.J. (2003). Coding of the contrasts in natural images by populations of neurons in primary visual cortex (V1). Vis. Res *43*, 1983–2001. https://doi.org/10.1016/s0042-6989(03)00277-3.

Conway, B.R., Hubel, D.H., and Livingstone, M.S. (2002). Color contrast in macaque V1. Cereb. Cortex *12*, 915–925. https://doi.org/10.1093/cercor/12.9.915.

Cox, M.A., Dougherty, K., Westerberg, J.A., Schall, M.S., and Maier, A. (2019). Temporal dynamics of binocular integration in primary visual cortex. J. Vis. *19*, 13. https://doi.org/10.1167/19.12.13.

Cumming, B.G., and DeAngelis, G.C. (2001). The physiology of stereopsis. Neuroscience *24*, 203–238. https://doi.org/10.1146/annurev.neuro.24.1.203.

DeAngelis, G.C., and Newsome, W.T. (1999). Organization of disparity-selective neurons in macaque area MT. J. Neurosci. *19*, 1398–1415. https://doi.org/10.1523/jneurosci.19-04-01398.1999.

Ding, J., Klein, S.A., and Levi, D.M. (2013a). Binocular combination of phase and contrast explained by a gain-control and gain-enhancement model. J. Vis. *13*, 13. https://doi.org/10.1167/13.2.13.

Ding, J., Klein, S.A., and Levi, D.M. (2013b). Binocular combination in abnormal binocular vision. J. Vis. *13*, 14. https://doi.org/10.1167/13.2.14.

Ding, J., and Levi, D.M. (2021). A unified model for binocular fusion and depth perception. Vis. Res *180*, 11–36. https://doi.org/10.1016/j.visres.2020.11.009.

Ding, J., and Levi, D.M. (2017). Binocular combination of luminance profiles. J. Vis. *17*, 4. https://doi.org/10.1167/17.13.4.

Ding, J., and Sperling, G. (2006). A gain-control theory of binocular combination. Proc. Natl. Acad. Sci. U S A. *103*, 1141–1146. https://doi.org/10.1073/pnas.0509629103.

Fleet, D.J., Wagner, H., and Heeger, D.J. (1996). Neural encoding of binocular disparity: energy models, position shifts and phase shifts. Vis. Res. *36*, 1839–1857. https://doi.org/10.1016/0042-6989(95)00313-4.

Freeman, R.D., and Ohzawa, I. (1990). On the neurophysiological organization of binocular vision. Vis. Res. *30*, 1661–1676. https://doi.org/10.1016/0042-6989(90)90151-a.

Georgeson, M.A., and Sengpiel, F. (2021). Contrast adaptation and interocular transfer in cortical cells: a re-analysis & a two-stage gain-control model of binocular combination. Vis. Res. *185*, 29–49. https://doi.org/10.1016/j.visres.2021.03.004.

Ghose, G.M., and Ts'O, D.Y. (1997). Form processing modules in primate area V4. J. Neurophysiol. *77*, 2191–2196. https://doi.org/10.1152/jn.1997.77.4.2191.

Giuseppe, N., and Andrea, F. (1983). Binocular interaction in visual-evoked responses: summation, facilitation and inhibition in a clinical study of binocular vision. Ophthalmic Res. *15*, 261–264. https://doi.org/10.1159/000265268.

Grünau, M.V. (1979). Binocular summation and the binocularity of cat visual cortex. Vis. Res. *19*, 813–816. https://doi.org/10.1016/0042-6989(79)90158-5.

Grünau, M.W., and Singer, W. (1979). The role of binocular neurons in the cat striate cortex in combining information from the two eyes. Exp. Brain Res. *34*, 133–142. https://doi.org/10.1007/bf00238346.

Haefner, R.M., and Cumming, B.G. (2008). Adaptation to natural binocular disparities in primate V1 explained by a generalized energy model. Neuron *57*, 147–158. https://doi.org/10.1016/j.neuron.2007.10.042.

Harter, M.R., Seiple, W.H., and Salmon, L. (1973). Binocular summation of visually evoked responses to pattern stimuli in humans. Vis. Res. *13*, 1433–1446. https://doi.org/10.1016/0042-6989(73)90004-7.

Henriksen, S., Tanabe, S., and Cumming, B. (2016). Disparity processing in primary visual cortex. Philosophical Trans. R. Soc B Biol. Sci. *371*, 20150255. https://doi.org/10.1098/rstb.2015.0255.

Heravian, J.S., Jenkins, T.C.A., and Douthwaite, W.A. (1990). Binocular summation in visually evoked responses and visual acuity. Ophthal Physl Opt. *10*, 257–261. https://doi.org/10.1111/j.1475-1313.1990.tb00861.x.

Heuer, H.W., and Britten, K.H. (2002). Contrast dependence of response normalization in area MT of the rhesus macaque. J. Neurophysiol. *88*, 3398–3408. https://doi.org/10.1152/jn.00255.2002.

Horton, J.C. (2006). Ocular integration in the human visual cortex. Can J. Ophthalmol. J. Can D'ophtalmologie *41*, 584–593. https://doi.org/10.1016/s0008-4182(06)80027-x.

Hou, C., Nicholas, S.C., and Verghese, P. (2020). Contrast normalization accounts for binocular interactions in human striate and extra-striate visual cortex. J. Neurosci. *40*, 2753–2763. https://doi.org/10.1523/jneurosci.2043-19.2020.

Huang, C.-B., Zhou, J., Zhou, Y., and Lu, Z.-L. (2010). Contrast and phase combination in binocular vision. PLoS One *5*, e15075. https://doi.org/10.1371/journal.pone.0015075.

Hubel, D.H., and Wiesel, T.N. (1962). Receptive fields, binocular interaction and functional architecture in the cat's visual cortex. J. Physiol. *160*, 106–154. https://doi.org/10.1113/jphysiol.1962.sp006837.

Legge, G.E. (1984). Binocular contrast summation—I. Detection and discrimination. Vis. Res *24*, 373–383. https://doi.org/10.1016/0042-6989(84)90063-4.

Lehky, S.R., and Maunsell, J.H.R. (1996). No binocular rivalry in the LGN of alert macaque monkeys. Vis. Res *36*, 1225–1234. https://doi.org/10.1016/0042-6989(95)00232-4.

Levelt, W.J.M. (1965). On binocular rivalry. On Binocular Rivalry (Inst. Perception Rvo-Tno).

Ling, S., and Blake, R. (2012). Normalization regulates competition for visual awareness. Neuron *75*, 531–540. https://doi.org/10.1016/j.neuron.2012.05.032.

Ling, S., and Carrasco, M. (2006). Sustained and transient covert attention enhance the signal via different contrast response functions. Vis. Res *46*, 1210–1220. https://doi.org/10.1016/j.visres.2005.05.008.

Livingstone, M.S., and Tsao, D.Y. (1999). Receptive fields of disparity-selective neurons in macaque striate cortex. Nat. Neurosci. *2*, 825–832. https://doi.org/10.1038/12199.

Longordo, F., To, M.-S., Ikeda, K., and Stuart, G.J. (2013). Sublinear integration underlies binocular processing in primary visual cortex. Nat. Neurosci. *16*, 714–723. https://doi.org/10.1038/nn.3394.

Maier, A., Wilke, M., Aura, C., Zhu, C., Ye, F.Q., and Leopold, D.A. (2008). Divergence of fMRI and neural signals in V1 during perceptual suppression in the awake monkey. Nat. Neurosci. *11*, 1193–1200. https://doi.org/10.1038/nn.2173.

Martinez-Trujillo, J.C., and Treue, S. (2002). Attentional modulation strength in cortical area MT depends on stimulus contrast. Neuron *35*, 365–370. https://doi.org/10.1016/s0896-6273(02)00778-x.

Matin, L. (1962). Binocular summation at the absolute threshold of peripheral vision. J. Opt. Soc. Am. *52*, 1276. https://doi.org/10.1364/josa.52.001276.

Maunsell, J.H., and Essen, D.C.V. (1983). Functional properties of neurons in middle temporal visual area of the macaque monkey. II. Binocular interactions and sensitivity to binocular disparity. J. Neurophysiol. *49*, 1148–1167. https://doi.org/10.1152/jn.1983.49.5.1148.

Meese, T.S., Georgeson, M.A., and Baker, D.H. (2006). Binocular contrast vision at and above threshold. J. Vis. *6*, 7. https://doi.org/10.1167/6.11.7.

Moradi, F., and Heeger, D.J. (2009). Inter-ocular contrast normalization in human visual cortex. J. Vis. *9*, 13. https://doi.org/10.1167/9.3.13.

Murphy, B.K., and Miller, K.D. (2003). Multiplicative gain changes are induced by excitation or inhibition alone. J. Neurosci. *23*, 10040–10051. https://doi.org/10.1523/jneurosci.23-31-10040.2003.

Nikara, T. (1972). Binocular vision of single units in the cat's striate cortex. Iyodenshi To Seitai Kogaku *10*, 80–87. https://doi.org/10.11239/jsmbe1963.10.80.

Ohzawa, I., Deangelis, G.C., and Freeman, R.D. (1997). Encoding of binocular disparity by complex cells in the cat's visual cortex. J. Neurophysiol. *77*, 2879–2909. https://doi.org/10.1152/jn.1997.77.6.2879.

Ohzawa, I., Sclar, G., and Freeman, R.D. (1985). Contrast gain control in the cat's visual system. J. Neurophysiol. *54*, 651–667. https://doi.org/10.1152/jn.1985.54.3.651.

Pachitariu, M., Steinmetz, N., Kadir, S., Carandini, M., and Harris Kenneth, D. (2016). Kilosort: realtime spike-sorting for extracellular electrophysiology with hundreds of channels. Preprint at bioRxiv. https://doi.org/10.1101/061481.

Pack, C.C., Born, R.T., and Livingstone, M.S. (2003). Two-dimensional substructure of stereo and motion interactions in macaque visual cortex. Neuron *37*, 525–535. https://doi.org/10.1016/s0896-6273(02)01187-x.

Pardhan, S., Gilchrist, J., Douthwaite, W., and Yap, M. (1990). Binocular inhibition: psychophysical and electrophysiological evidence. Optom. Vis. Sci *67*, 688–691. https://doi.org/10.1097/00006324-199009000-00006.

Parker, A.J., and Cumming, B.G. (2001). Chapter 14 Cortical mechanisms of binocular stereoscopic vision. Prog. Brain Res. *134*, 205–216. https://doi.org/10.1016/s0079-6123(01)34015-3.

Parker, A.J., Smith, J.E.T., and Krug, K. (2016). Neural architectures for stereo vision. Philos. Trans. R. Soc B Biol. Sci *371*, 20150261. https://doi.org/10.1098/rstb.2015.0261.

Pettigrew, J.D., Nikara, T., and Bishop, P.O. (1968). Binocular interaction on single units in cat striate cortex: simultaneous stimulation by single moving slit with receptive fields in correspondence. Exp. Brain Res. *6*, 391–410. https://doi.org/10.1007/bf00233186.

Pirenne, M.H. (1943). Binocular and uniocular threshold of vision. Nature *152*, 698–699. https://doi.org/10.1038/152698a0.

Poggio, G.F. (1995). Mechanisms of stereopsis in monkey visual cortex. Cereb. Cortex *5*, 193–204. https://doi.org/10.1093/cercor/5.3.193.

Poggio, G.F., and Fischer, B. (1977). Binocular interaction and depth sensitivity in striate and prestriate cortex of behaving rhesus monkey. J. Neurophysiol. *40*, 1392–1405. https://doi.org/10.1152/jn.1977.40.6.1392.

Qian, C.S., and Brascamp, J.W. (2017). How to build a dichoptic presentation system that includes an eye tracker. J. Vis. Exp. Jove *127*, e56033. https://doi.org/10.3791/56033.

Read, J.C.A., and Cumming, B.G. (2003). Testing quantitative models of binocular disparity selectivity in primary visual cortex. J. Neurophysiol. *90*, 2795–2817. https://doi.org/10.1152/jn.01110.2002.

Read, J.C.A., Parker, A.J., and Cumming, B.G. (2002). A simple model accounts for the response of disparity-tuned V1 neurons to anticorrelated images. Vis. Neurosci *19*, 735–753. https://doi.org/10.1017/s0952523802196052.

Said, C.P., and Heeger, D.J. (2013). A model of binocular rivalry and cross-orientation suppression. Plos Comput. Biol. *9*, e1002991. https://doi.org/10.1371/journal.pcbi.1002991.

Salthouse, T.A., and Ellis, C.L. (1980). Determinants of eye-fixation duration. Am. J. Psychol. *93*, 207–234.

Schroeder, C.E., Tenke, C.E., Arezzo, J.C., and Vaughan, H.G. (1990). Binocularity in the lateral geniculate nucleus of the alert macaque. Brain Res. *521*, 303–310. https://doi.org/10.1016/0006-8993(90)91556-v.

Sclar, G., Ohzawa, I., and Freeman, R.D. (1986). Binocular summation in normal, monocularly deprived, and strabismic cats: visual evoked potentials. Exp. Brain Res. *62*, 1–10. https://doi.org/10.1007/bf00237398.

Sengpiel, F., Baddeley, R.J., Freeman, T.C.B., Harrad, R., and Blakemore, C. (1998). Different mechanisms underlie three inhibitory phenomena in cat area 17. Vis. Res *38*, 2067–2080. https://doi.org/10.1016/s0042-6989(97)00413-6.

Sengpiel, F., and Blakemore, C. (1994). Interocular control of neuronal responsiveness in cat visual cortex. Nature *368*, 847–850. https://doi.org/10.1038/368847a0.

Smith, E.L., Chino, Y., Ni, J., and Cheng, H. (1997). Binocular combination of contrast signals by striate cortical neurons in the monkey. J. Neurophysiol. *78*, 366–382. https://doi.org/10.1152/jn.1997.78.1.366.

Summa, A., Polo, A., Tinazzi, M., Zanette, G., Bertolasi, L., Bongiovanni, L.G., and Fiaschi, A. (1997). Binocular interaction in normal vision studied by pattern-reversal visual evoked potentials (PR-VEPS). Ital. J Neurol. Sci *18*, 81–86. https://doi.org/10.1007/bf01999567.

Tanabe, S., and Cumming, B.G. (2008). Mechanisms underlying the transformation of disparity signals from V1 to V2 in the macaque. J. Neurosci. *28*, 11304–11314. https://doi.org/10.1523/jneurosci.3477-08.2008.

Thiele, A., Pooresmaeili, A., Delicato, L.S., Herrero, J.L., and Roelfsema, P.R. (2009). Additive effects of attention and stimulus contrast in primary visual cortex. Cereb. Cortex New York Ny *19*, 2970–2981. https://doi.org/10.1093/cercor/bhp070.

Tsang, E.K.C., and Shi, B.E. (2008). Normalization enables robust validation of disparity estimates from neural populations. Neural Comput. *20*, 2464–2490. https://doi.org/10.1162/neco.2008.05-07-532.

Westerberg, J.A., Cox, M.A., Dougherty, K., and Maier, A. (2019). V1 microcircuit dynamics: altered signal propagation suggests intracortical origins for adaptation in response to visual repetition. J. Neurophysiol. *121*, 1938–1952. https://doi.org/10.1152/jn.00113.2019.

Yang, Y., Liu, S., Chowdhury, S.A., DeAngelis, G.C., and Angelaki, D.E. (2011). Binocular disparity tuning and visual-vestibular congruency of multisensory neurons in macaque parietal cortex. J. Neurosci. *31*, 17905–17916. https://doi.org/10.1523/jneurosci.4032-11.2011.

Yehezkel, O., Ding, J., Sterkin, A., Polat, U., and Levi, D.M. (2016). Binocular combination of stimulus orientation. Roy Soc. Open Sci. *3*, 160534. https://doi.org/10.1098/rsos.160534.

Zhao, X., Liu, M., and Cang, J. (2013). Sublinear binocular integration preserves orientation selectivity in mouse visual cortex. Nat. Commun. *4*, 2088. https://doi.org/10.1038/ncomms3088.

STAR★METHODS

KEY RESOURCES TABLE

REAGENT or RESOURCE	SOURCE	IDENTIFIER
Deposited data		
Post-processing MATLAB code	This paper	Zenodo: https://doi.org/10.5281/zenodo.6371744
Experimental models: Organisms/strains		
Bonnet macaque (*Macaca radiata*)	Wake Forest University, North Carolina, USA	N/A
Software and algorithms		
MATLAB, 2012-2014 and 2016A	MathWorks	https://www.mathworks.com/
MonkeyLogic	David Freedman, University of Chicago; Wael Assad, Brown University	http://www.brown.edu/Research/monkeylogic/
KiloSort	(Pachitariu et al., 2016)	https://github.com/cortex-lab/KiloSort
Jamovi, v2.0.0	The jamovi project, and Sebastian Jentschke	https://www.jamovi.org/
Other		
Vector Array	NeuroNexus	http://neuronexus.com/products/neural-probes/
U-Probe, V-Probe	Plexon Inc	https://plexon.com/
Recording equipment	Blackrock Microsystems	http://blackrockmicro.com/
Eye Link II Eye Tracker	SR Research	https://www.sr-research.com/
Cold mirrors	Edmund Optics	https://www.edmundoptics.com/
Data Acquisition Board PCI-6229	National Instruments	http://www.ni.com/en-us.html
Eye-tracking Software	SensoMotoric Instruments	https://www.smivision.com/
Photodiode	OSI Optoelectronics	http://www.osioptoelectronics.com/
Ceramic screws	Thomas Recording	https://www.thomasrecording.com/
Dental Acrylic	Lang Dental Manufacturing	http://www.orthodonticproductsonline.com/buyers-guide/listing/lang-dental-manufacturing-co-inc/
Microdrive	Narishige International USA, Inc.	https://usa.narishige-group.com/
Plastic Recording Chamber	Crist Instrument; custom-made	http://www.cristinstrument.com/;Vanderbilt University

RESOURCE AVAILABILITY

Lead contact

Further information and requests for resources and reagents should be directed to and will be fulfilled by the lead contact, Blake A. Mitchell (blake.a.mitchell@vanderbillt.edu).

Materials availability

This study did not generate new unique materials. All materials found in the key resource table may be obtained commercially.

Data and code availability

- All data reported in this paper will be shared by the lead contact upon request.
- All original code has been deposited at Zenodo and is publicly available as of the date of publication.
- Any additional information required to reanalyze the data reported in this paper is available from the lead contact upon request.

EXPERIMENTAL MODEL AND SUBJECT DETAILS

Two adult monkeys (Monkey E48, male, age 9; I34, female, age 12; *Macaca radiata*) were used in this study. We report on neurophysiological data recorded during 19 penetrations (14 in Monkey E48) of area V1. All procedures followed regulations by the Association for the Assessment and Accreditation of Laboratory Animal Care (AALAC), Vanderbilt University's Institutional Animal Care and Use Committee (IACUC), and National Institutes of Health (NIH) guidelines.

METHOD DETAILS

Surgical procedures

Prior to data collection, animals were implanted with a custom-designed plastic head holder and a plastic recording chamber (Crist Instruments) spanning over two separate surgeries. All surgeries were performed under sterile surgical conditions using isoflurane anesthesia (1.5–2.0%). Vital signs, including heart rate, blood pressure, SpO_2, CO_2, body temperature, and respiratory rate were monitored continuously. During surgery, the head holder and a recording chamber were attached to the skull using transcranial ceramic screws (Thomas Recording, Gießen, Germany) and self-curing dental acrylic (Lang Dental Manufacturing, Wheeling, IL). A craniotomy was performed over the parafoveal visual field representation of primary visual cortex (V1) concurrent with the position of the recording chamber. Animals received analgesics and antibiotics for postsurgical care and closely monitored by researchers, facility veterinarians, and animal care staff for at least three days following surgery.

Visual apparatus

Stimuli were presented on a linearized CRT monitor running at either 60 Hz (resolution 1,280 × 1,024 pixels) or 85 Hz (resolution 1,024 × 768). Animals viewed all stimuli through a custom-built mirror stereoscope, such that images on the right side of the display were viewed by the right eye and images on the left by the left eye (Figure 1A; the monitor was divided by a black, nonreflective septum). The mirrors of the stereoscope were infrared-transparent (Qian and Brascamp, 2017), enabling gaze position to be measured using infrared light-sensitive cameras (EyeLink II). To facilitate binocular fusion, an oval aperture was displayed at the edge of each half of the screen. At the beginning of each experimental session, the stereoscope was calibrated via a behavioral task (Maier et al., 2008), which required the animals to fixate on the same location in visual space while being cued in one eye only. Gaze position was measured for each fixation location and compared across eyes. When gaze position was comparable for cueing in each eye, the mirrors were considered aligned.

Behavioral task

A trial began once the animal fixated (self-initiated) within 1° of visual angle of a centralized fixation cue appearing in both eyes. A series of sinusoidal grating stimuli were presented to the left eye, right eye, or both eyes at a fixed location in parafoveal visual space, each lasting 250-500 ms with a 500 ms interval interleaved (details of stimuli are described later). If fixation was held for the duration of the trial, the monkey received a juice reward. Alternatively, the next fixation cue appeared with a brief (1-5 s) delay. The animals were at liberty to end recording sessions at any point by halting the initiation of new trials. No other behavior was required.

Neurophysiological procedure

Experiments were conducted inside a radio frequency-shielded booth. During each recording session, a linear multielectrode array (U-Probe, Plexon Inc., Dallas, TX; Vector Array, NeuroNexus, Ann Arbor, MI) was inserted into V1 orthogonal to the cortical surface. Fluctuating extracellular voltages (referenced to the metallic electrode shaft) were amplified, filtered, and digitized using a 128-channel Cerebus neural signal processing system (Blackrock Microsystems, Salt Lake City, UT). Two neural signals were recorded and stored for subsequent offline analysis: a low-pass filtered signal (0.3–500 Hz) sampled at 1 kHz, corresponding to the local field potential, or LFP, and a broadband (0.3 Hz–7.5 kHz) signal sampled at 30 kHz. The neural signal processing system also recorded non-neurophysiological analog signals related to the monitor refresh (i.e., a photodiode signal; OSI Optoelectronics, Montreal, Quebec) and eye position (i.e., voltage output of eye-tracking system), which were digitized and stored at 30 and 1 kHz, respectively. These time stamps and the photodiode signal were used to align the time-varying intracranial data with the occurrence of visual events.

During recording session, the parameters of the sinusoidal grating stimuli (orientation, phase, spatial frequency, location, etc.) were customized relative to the receptive field and tuning preferences of the

population of neurons recorded across the microelectrode array. Details of these procedures, including the reverse correlation-like receptive field mapping procedure and the paradigms used to identify tuning preferences have been described in detail previously (Cox et al., 2019; Westerberg et al., 2019). Note, all receptive fields were mapped binocularly, and receptive fields for a given penetration always overlapped due to the orthogonal angle of the microelectrode array to V1.

Pre-processing of spiking activity

Offline, we computed a discretized measure of multi-unit activity (MUA) by applying a time-varying threshold to the envelope of the broadband signal, with an impulse recorded at every time point where the signal envelope exceeded the threshold on each microelectrode contact. Single-unit activity was extracted using Kilosort, an unsupervised machine-learning spike-sorting algorithm (Pachitariu et al., 2016). Both techniques have been described in detail previously (Cox et al., 2019). Here, all analyses were conducted on the discretized multi-unit activity unless otherwise stated. To be included in this study, the spiking units had to fall within the bounds of V1 and exhibit a significant response to visual stimulation, determined by performing a paired-samples *t* test ($\alpha = 0.05$) on the mean baseline activity on each trial and the mean activity during the epoch of visual stimulation (0-250 ms).

QUANTIFICATION AND STATISTICAL ANALYSIS

V1 responses to monocular and binocular stimulation

For our purposes here, we analyzed spiking responses to stimulation of one or the other eye (monocular) or stimulation of both eyes simultaneously (binocular). All stimuli of these trials consisted of sinusoidal, monochromatic gratings. Features of the gratings, such as size, spatial frequency, and orientation, were set to values which elicited the strongest spiking response of the V1 population, informed by unit responses collected in the tuning paradigms (see Neurophysiological Procedure and Supp. Figure). For binocular presentation of gratings, all parameters (size, orientation, spatial frequency, and contrast) were identical between the two eyes and positional disparity was set to zero (resulting in an actual disparity close to zero given the flat surface of the monitor relative to the curvature of the horopter). Throughout the paper, we use the term *monocular* for all stimuli consisting of a grating of the units' preferred orientation, presented to either the left or right eye in isolation. We use the term *dioptic* (*binocular*) to refer to the condition where the same grating is presented at corresponding retinal points to both eyes.

The stimulus parameter that varied experimentally was the Michelson contrast of the grating(s) between presentations. The exact contrast levels used across recording days varied slightly (e.g., we sampled responses to more, evenly spaced, contrasts on days where the animals' motivation was high). We thus grouped the following contrast ranges: [0, 0.20-0.225, 0.40-0.45, 0.80-0.90].

Duration of binocular facilitation

Duration of binocular facilitation was evaluated in efforts to assess contrast-dependency of binocular modulation across time. For this analysis, we estimated the onset and offset of facilitation from each unit's delta spiking response (250 ms). We estimated the onset of facilitation as the timepoint associated with the peak magnitude of facilitation for each unit. We estimated the offset of facilitation for each unit by identifying the timepoint after onset at which the delta response crossed zero. Duration was then computed as offset minus onset of facilitation. This procedure was repeated for each stimulus contrast level. Since we were only interested the temporal dynamics of facilitation, units that did not show facilitation (positive delta) at any timepoint were excluded from this analysis (n = 32).

Determining ocular dominance

Our analysis aimed to compare binocular responses of V1 neurons to their monocular counterparts. Neurons in V1 are known to differ in the magnitude they respond to stimuli presented to one eye or the other (Hubel and Wiesel, 1962). This is the *ocular dominance* of the neuron. We used the neuronal responses to monocular stimulation to compute an ocularity index that quantifies a unit's selectivity for one versus the other eye,

$$\text{ocularity} = \frac{mean(LE) - mean(RE)}{mean(LE) + mean(RE)}$$

defined as differences between trial-averaged responses (*mean*, 0-250 ms) of each eye divided by their sum. All nonrelevant parameters, such as orientation and contrast, were matched for this process. For each unit, we used this value to distinguish "dominant (DE) eye" and "non-dominant (NDE)".

Contrast response functions (CRFs)

Contrast response functions (CRFs) portray a neuron's mean spiking response as a function of stimulus contrast (Albrecht and Hamilton, 1982). To determine how binocular V1 spiking responses vary as a function of contrast, we measured CRFs in units for which there was four datapoints (247 in monkey E, 8 in monkey I) under monocular and binocular stimulation (Figures 1G and 1H). Trial-averaged spiking responses (over varying time windows) as a function of visual contrast were fit using the Naka-Rushton function:

$$R_{R_{max},\ C_{50},\ n,\ b}(c) = \frac{Rmax * \ c^n}{c^n + {C_{50}}^n} + b$$

where R is the response of the unit, R_{max} is the projected maximum response of the unit, C_{50} is the semi-saturation constant that represents the contrast at which the output is half of the maximum response, n is the scaling exponent, and c is the contrast of the stimulus. The y-intercept b represents the maintained activity and was fixed for individual neurons to the average activity during blank trials (0 contrast = gray background). The parameters R_{max}, C_{50}, and n collectively determine the shape of the contrast response curve (Carandini and Heeger, 2012). For each unit, the trial-averaged contrast responses under binocular and monocular conditions were fit with all parameters free to vary [R_{max}, C_{50}, n].

Statistical analysis

We used custom code written in Matlab (The Mathworks Inc.) for data analysis. All statistical analysis were conducted in Jamovi version 2.0.0, an open-source statistical software. Mean piking responses (N = 314 units, 234 from Monkey E) to stimuli of varying contrast [0, 0.20-0.225, 0.40-0.45, 0.80-0.90] were compared across monocular and binocular stimulation. Mean responses were either taken as time-average spiking across full stimulus presentation (0-250 ms) or 100 ms windows within this timeframe, as noted. Data from monkey "I" had incomplete observations at low and medium contrast (see Table 1 for sample information), which prevented the use of repeated measures ANOVA on pooled units from both animals. To test effects of stimulus contrast across both animals without discarding data, we employed a mixed-model analysis of variance with contrast as a continuous predictor and the unit as a random factor (Figures 1 and 2). Subsequent analyses employed repeated measures ANOVA on units with complete observations (Figures 3, 4, and 5). Post hoc tests were performed when appropriate to test for significant ($p < 0.05$) contrasts between samples (two-tailed, paired t tests) with Bonferonni correction. Performance of simple models of gain-control were evaluated by goodness of fit (R^2) to the observed binocular contrast responses (mean spiking over 100 ms windows).